Article

Cu Binding Modes of Recombinant #-Synuclein # Insights from EPR Spectroscopy

Simon C. Drew, Su Ling Leong, Chi L. L. Pham, Deborah J. Tew, Colin L. Masters, Luke A. Miles, Roberto Cappai, and Kevin J. Barnham

J. Am. Chem. Soc., **2008**, 130 (24), 7766-7773 • DOI: 10.1021/ja800708x • Publication Date (Web): 22 May 2008

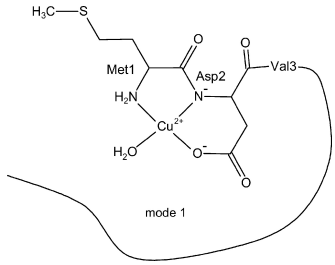

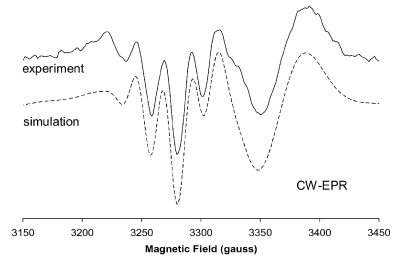

More About This Article

Additional resources and features associated with this article are available within the HTML version:

- Supporting Information
- Access to high resolution figures
- Links to articles and content related to this article
- Copyright permission to reproduce figures and/or text from this article

View the Full Text HTML

J|A|C|S
ARTICLES

Published on Web 05/22/2008

Cu^{2+} Binding Modes of Recombinant α-Synuclein − Insights from EPR Spectroscopy

Simon C. Drew,[†,‡,§,||] Su Ling Leong,[†,‡] Chi L. L. Pham,[†,‡,§] Deborah J. Tew,[†,‡,§] Colin L. Masters,[§,⊥] Luke A. Miles,[○] Roberto Cappai,[†,‡,§] and Kevin J. Barnham*[,†,‡,§]

Department of Pathology, Bio21 Molecular Science and Biotechnology Institute, and Centre for Neuroscience, The University of Melbourne, Victoria 3010, Australia, School of Physics, Monash University, Victoria 3800, Australia, The Mental Health Research Institute, Victoria 3052, Australia, and Graduate School of Science, Tokyo Metropolitan University, 1-1 minami-ohsawa, Hachioji, 192-0397, Japan

Received January 29, 2008; E-mail: kbarnham@unimelb.edu.au

Abstract: The interaction of the small (140 amino acid) protein, α-synuclein (αS), with Cu^{2+} has been proposed to play a role in Parkinson's disease (PD). While some insight from truncated model complexes has been gained, the nature of the corresponding Cu^{2+} binding modes in the full length protein remains comparatively less well characterized. This work examined the Cu^{2+} binding of recombinant human αS using Electron Paramagnetic Resonance (EPR) spectroscopy. Wild type (wt) αS was shown to bind stoichiometric Cu^{2+} via two N-terminal binding modes at physiological pH. An H50N mutation isolated one binding mode, whose $g_{||}$, $A_{||}$, and metal−ligand hyperfine parameters correlated well with a {NH_2, N^-, β-COO^-, H_2O} mode previously identified in truncated model fragments. Electron spin−echo envelope modulation (ESEEM) studies of wt αS confirmed the second binding mode at pH 7.4 involved coordination of His50 and its $g_{||}$ and $A_{||}$ parameters correlated with either {NH_2, N^-, β-COO^-, N_{Im}} or {N_{Im}, $2N^-$} coordination observed in αS fragments. At pH 5.0, His50-anchored Cu^{2+} binding was greatly diminished, while {NH_2, N^-, β-COO^-, H_2O} binding persisted in conjunction with another two binding modes. Metal−ligand hyperfine interactions from one of these indicated a 1N3O coordination sphere, which was ascribed to a {NH_2, CO} binding mode. The other was characterized by a spectrum similar to that previously observed for diethylpyrocarbonate-treated αS and was attributed to C-terminal binding centered on Asp121. In total, four Cu^{2+} binding modes were identified within pH 5.0−7.4, providing a more comprehensive picture of the Cu^{2+} binding properties of recombinant αS.

Introduction

The 140 amino acid presynaptic protein α-synuclein (αS) is implicated in many neurodegenerative diseases including Parkinson's disease (PD), dementia with Lewy bodies, and the Lewy body variant of Alzheimer's disease.[1,2] The central role of αS in PD is highlighted by the association of three mutations (A30P, E46K, A53T) with the familial forms of the disease [3–5] and the presence of αS aggregates in the cytoplasmic inclusions (Lewy bodies) of diseased dopaminergic neurons. However, the specific mechanism by which αS contributes to PD remains unclear.

αS is predominantly localized at presynaptic terminals, where it is thought to play a role in modulating synaptic plasticity, neurotransmitter release, presynaptic vesicle recycling, and pool size.[1] The N-terminus of αS is comprised of several 11-amino acid repeats, whose amphiphilic character renders the protein readily exchangeable between membrane and aqueous media.[6,7] Studies on synthetic membranes have shown that αS binds preferentially to small unilamellar vesicles containing acidic phospholipids,[8] causing the N-terminal residues (1−102) to undergo a structural change from a natively unfolded conformation to an α-helix-rich conformation, while the negatively charged C-terminus remains mobile and solvent accessible.[6,9,10] The membrane-bound form has a higher tendency to aggregate

† Department of Pathology, The University of Melbourne.
‡ Bio21 Molecular Science and Biotechnology Institute, The University of Melbourne.
§ The Mental Health Research Institute.
|| School of Physics, Monash University.
⊥ Centre for Neuroscience.
○ Graduate School of Science, Tokyo Metropolitan University.

(1) Burke, R. E. *Neurologist* **2004**, *10*, 7581 and references therein.
(2) Rochet, J. C.; Outeiro, T. F.; Conway, K. A.; Ding, T. T.; Volles, M. J.; Lashuel, H. A.; Bieganski, R. M.; Lindquist, S. L.; Lansbury, P. T. *J. Mol. Neurosci.* **2004**, *23*, 23–34.
(3) Krüger, R.; Kuhn, W.; Müller, T.; Woitalla, D.; Graeber, M.; Kösel, S.; Przuntek, H.; Epplen, J. T.; Schöls, L.; Riess, O. *Nat. Genet.* **1998**, *18*, 106–108.
(4) Polymeropoulos, M. H., et al. *Science* **1997**, *276*, 2045–2047.
(5) Zarranz, J. J.; Alegre, J.; Gómez-Esteban, J. C.; Lezcano, E.; Ros, R.; Ampuero, I.; Vidal, L.; Hoenicka, J.; Rodriguez, O.; Atarés, B.; Llorens, V.; Tortosa, E. G.; del Ser, T.; Muñoz, D. G.; de Yebenes, J. G. *Ann. Neurol.* **2004**, *55*, 164–173.
(6) Bussell Jr, R.; Eleizer, D. *J. Mol. Biol.* **2003**, *329*, 763–778.
(7) Bisaglia, M.; Tessari, I.; Pinato, L.; Bellanda, M.; Giraudo, S.; Fasano, M.; Bergantino, E.; Bubacco, L.; Mammi, S. *Biochemistry* **2005**, *44*, 329–339.
(8) Davidson, W. S.; Jonas, A.; Clayton, D. F.; George, J. M. *J. Biol. Chem.* **1998**, *273*, 9443–9449.
(9) Ramakrishnan, M.; Jensen, P. H.; Marsh, D. *Biochemistry* **2003**, *42*, 12919–12926.
(10) Perrin, R. J.; Woods, W. S.; Clayton, D. F.; George, J. M. *J. Biol. Chem.* **2000**, *275*, 34393–34398.

 10.1021/ja800708x CCC: $40.75

than the cytosolic form, with the membrane-bound aggregates being able to seed accelerated aggregation of the cytosolic form.[11] These properties have been linked to intracellular cytotoxic effects of αS.

The presence of αS in presynaptic terminals places it in a cytosolic, and hence highly reducing, environment that favors Cu^{+} coordination over Cu^{2+}. However, a small proportion of αS monomers and aggregates are also secreted by neuronal cells into extracellular environments that favor Cu^{2+} binding, including the cerebrospinal fluid[12,13] and plasma.[14,15] Divalent copper can accelerate the rate of αS fibrilization *in vitro*, even at physiological concentrations of Cu^{2+},[16] and extracellular αS aggregates are toxic to cultured neuronal cells.[17] The αS fragment (residues 61−95), known as the nonamyloid-β (Aβ) component, is also found in the extracellular plaques associated with aggregates of the Aβ peptide in Alzheimer's disease (AD), where Cu^{2+}-Aβ mediated production of reactive oxygen species has been proposed to contribute to the oxidative cell damage observed in AD.[18] Like Aβ, recombinant αS is capable of generating hydrogen peroxide *in vitro* in the presence of trace Cu^{2+},[19,20] while residues in the vicinity of coordinated Cu^{2+} in model fragments of αS are oxidatively modified in the presence of hydrogen peroxide.[21,22] In a rat model of PD, oral administration of the metal binding compound 5-chloro-7-iodo-8-hydroxyquinoline (clioquinol) was found to significantly reduce susceptibility to 1-methyl-4-phenyl-1,2,3,6-tetrapyridine (MPTP), an agent which causes PD-like symptoms.[23] These observations suggest that Cu^{2+}−αS interactions may be directly relevant to understanding the pathological processes that lead to PD and highlight the need for a detailed understanding of the Cu^{2+} binding properties of αS.

Estimates suggest αS can bind Cu^{2+} with an affinity of $K_d = 0.12 \pm 0.16\ \mu M$ in the N-terminus and $K_d = 36 \pm 36\ \mu M$ in the C-terminus[16] (although the large errors leave these values poorly defined). C-terminal Cu^{2+} binding has been implicated in the aggregation of membrane-associated αS.[24] The C-terminus further appears capable of binding other divalent metal ions such as Co^{2+}, Mn^{2+}, Ni^{2+}, and Fe^{2+}; however the affinity for these metal ions was reported to be very low ($K_d \sim 1$ mM)[25] and is therefore unlikely to be physiologically relevant. Ca^{2+} can also bind to the C-terminus and facilitate oligomerization.[26]

Initial spectroscopic studies of Cu^{2+} binding by recombinant αS at pH 6.5 suggested that the Cu^{2+} binding could be wholly attributed to a single coordination mode involving a macrochelate between the N-terminus and the imidazole side chain of His50.[16] Paramagnetic broadening of the NMR signals from the wild-type protein at pH 5.0 indicated that the acidic C-terminus was able to coordinate Cu^{2+} in the vicinity of residues 119−123. By comparison with the EPR spectrum at pH 5.0, the residual EPR spectrum following diethylpyrocarbonate (DEPC) treatment was also ascribed to the C-terminal Cu^{2+} binding site and assigned a 4O coordination sphere centered on Asp121.[16] However, evidence of a metal−ligand superhyperfine (shf) structure was apparent, which cannot occur for coordination by oxygen ligands alone due to their zero nuclear magnetic moment (nat. abundance >99.5% ^{16}O, $I = 0$).

The existence of cooperative Cu^{2+} binding by the N-terminus and His50 was later disputed. An NMR study demonstrated that paramagnetic broadening due to Cu^{2+} binding was not eliminated at the N-terminus in an H50A mutant, suggesting that the N-terminus could bind Cu^{2+} independently of His50 and hence that macrochelate formation did not occur.[27] However, the demonstration of the ability of the N-terminus to bind Cu^{2+} via a mode not incorporating His50 does not preclude the presence of other Cu^{2+} binding modes which do. Indeed, two dominant binding modes of the form $\{NH_2, N^-, \beta\text{-}COO^-, H_2O\}$ and $\{NH_2, N^-, \beta\text{-}COO^-, N_{im}\}$ were suggested from potentiometric and spectroscopic studies of truncated model αS fragments M^{29}-D^{30}-56 and M^{26}-D^{27}-56(A30P,A53T) at physiological pH.[22,28–30] While such studies have provided a model of Cu^{2+} binding by the N-terminus of αS over a wide pH range, the applicability of these findings is yet to be confirmed for the *bona fide* protein.

The above results show that the earlier spectroscopic characterization of recombinant αS was incomplete and further highlight the need to reconcile the Cu^{2+} binding properties of the full length protein with the spectroscopic and potentiometric analyses performed on model peptide fragments. This study therefore employed CW- and pulsed-EPR, together with site-directed mutagenesis and isotopic labeling, to investigate the aqueous Cu^{2+} binding modes of recombinant human αS. The key binding modes at pH 5.0 and pH 7.4 were spectrally

(11) Lee, H-J.; Choi, C.; Lee, S-J. *J. Biol. Chem.* **2002**, *277*, 671–678.
(12) Borghia, R.; Marcheseb, R.; Negroc, A.; Marinellia, L.; Forlonid, G.; Zaccheoa, D.; Abbruzzeseb, G.; Tabatona, M. *Neurosci. Lett.* **2000**, *287*, 65–67.
(13) Lee, H-J.; Patel, S.; Lee, S-J. *J. Neurosci.* **2005**, *25*, 6016–6024.
(14) El-Agnaf, O. M.; Salem, S. A.; Paleologou, K. E.; Cooper, L. J.; Fullwood, N. J.; Gibson, M. J.; Curran, M. D.; Court, J. A.; Mann, D. M. A.; Ikeda, S.; Cookson, M. R.; Hardy, S.; Allsop, D. *FASEB J.* **2003**, *17*, 1945–1947.
(15) Li, Q-X.; Mok, S. S.; Laughton, K. M.; McLean, C. A.; Cappai, R.; Masters, C. L.; Culvenor, J. G.; Horne, M. K. *Exp. Neurol.* **2007**, *204*, 583–588.
(16) Rasia, R. M.; Bertoncini, C. W.; Marsh, D.; Hoyer, W.; Cherny, D.; Zweckstetter, M.; Griesinger, C.; Jovin, T. M.; Fernández, C. O. *Proc. Natl. Acad. Sci. U.S.A.* **2005**, *102*, 4294–4299.
(17) El-Agnaf, O. M. A.; Jakes, R.; Curran, M. D.; Middleton, D.; Ingenito, R.; Bianchi, E.; Pessi, A.; Neille, D.; Wallace, A. *FEBS Lett.* **1998**, *440*, 71–75.
(18) Barnham, K. J.; Masters, C. L.; Bush, A. I. *Nat. Rev. Drug Discovery* **2004**, *3*, 205–214.
(19) Turnbull, S.; Tabner, B. J.; El-Agnaf, O. M. A.; Moore, S.; Davies, Y.; Allsop, D. *Free Radical Biol. Med.* **2002**, *30*, 1163–1170.
(20) Tabner, B. J.; Turnbull, S.; El-Agnaf, O. M. A.; Allsop, D. *Free Radical Biol. Med.* **2002**, *32*, 1076–1083.
(21) Kowalik-Jankowska, T.; Rajewska, A.; Jankowska, E.; Wiśniewska, K.; Grzonka, Z. *J. Inorg. Biochem.* **2006**, *100*, 1623–1631.
(22) Kowalik-Jankowska, T.; Rajewska, A.; Jankowska, E.; Grzonka, Z. *Dalton Trans.* **2007**, 4197–4206.
(23) Kaur, D., et al. *Neuron* **2003**, *37*, 899–909.
(24) Lee, N.; Lee, S. Y.; Lee, D.; Kim, J.; Paik, S. R. *J. Neurochem.* **2003**, *84*, 1128–1142.
(25) Binolfi, A.; Rasia, R. M.; Bertoncini, C. W.; Ceolin, M.; Zweckstetter, M.; Griesinger, C.; Jovin, T. M.; Fernández, C. O. *J. Am. Chem. Soc.* **2006**, *128*, 9893–9901.
(26) Lowe, R.; Pountney, D. L.; Jensen, P. H.; Gai, W. P.; Voelcker, N. H. *Protein Sci.* **2004**, *13*, 3245–3252.
(27) Sung, Y.; Rospigliosi, C.; Eliezer, D. *Biochim. Biophys. Acta* **2006**, *1764*, 5–12.
(28) Kowalik-Jankowska, T.; Rajewska, A.; Jankowska, E.; Grzonka, Z. *Dalton Trans.* **2006**, 5068–5076.
(29) M^{29}-D^{30}-56=NH_2-M^{29}-D^{30}-GKTKEGVLYV^{40}GSKTKEGVVH^{50}GVATVA^{56}-NH_2). M^{26}-D^{27}-56(A30P,A53T) = NH_2-M^{26}-D^{27}-EA***P***GKTKEGV-LYV^{40}GSKTKEGVVH^{50}GV***T***TVA^{56}-NH_2). The role of Met1 and Asp2 residues in the full length protein was modeled by appending a Met-Asp sequence to the N-terminus of the model complexes.
(30) Here, the $\{NH_2, N^-, \beta\text{-}COO^-, N_{Im}\}$ coordination was suggested to be comprised of two separate contributions at physiological pH, one mode involving additional coordination via an ϵ-amino nitrogen from a Lys side chain in the apical position. This axial coordination has little impact on the EPR spectrum, and their spin Hamiltonian parameters in the model complex are effectively indistinguishable. See ref 28.

isolated, simulated, and compared with existing experimental data to provide a more detailed description of Cu^{2+} binding by full length αS in the aqueous state. Such a description is fundamental to understanding the potential role of metals in Parkinson's disease.

Method

Recombinant aS Expression and Purification. Human αS cDNA was cloned into pRSETB plasmid (Invitrogen, Carlsbad, CA) and transformed into *Escherichia coli* BL21(DE3) competent cells (Invitrogen, Carlsbad, CA). Overexpression was induced with 1 mM IPTG. Cells were harvested by centrifugation followed by sonication in lysis buffer (20 mM Tris, 1 mM EDTA, pH 7.5) containing protease inhibitor tablets (Pierce). αS was purified according to Cappai et al.[31] The H50N mutant was generated via Quikchange site directed mutagenesis kit (Stratagene). The expression and purification of H50N was performed as described for WT αS.

Overexpression of isotopic ^{15}N-labeled αS was performed according to Marley et al.[32] Briefly, BL21(DE3) cells containing αS-pRSETB expression plasmid was initially grown in rich LB media until midlog phase ($OD_{600nm} = 0.6$). Cells were centrifuged and exchanged into minimal media[33] containing $^{15}NH_4Cl$ (98% ^{15}N; Cambridge Isotope Laboratories). Cell growth was allowed to recover by incubating at 37 °C for 1 h before expression was induced overnight with 1 mM IPTG. Cells were harvested and purified according to the protocol used for unlabeled αS.

EPR Sample Preparation. 1 mg of lyophilized αS was resuspended in 150 μL of PBS 7.4 (Amresco), mixed vigorously, and then placed in a sonicating water bath (Ultrasonics, Australia) for 15 min to fully solubilize the protein. The concentration was determined from the optical density at 280 nm using an extinction coefficient of 5120 M^{-1} cm^{-1} and adjusted to ca. 350 μM with 1 × PBS. From a 10 mM stock of $^{65}CuCl_2$, prepared from ^{65}CuO (Cambridge Isotope Laboratories) in HCl, 1 equiv of $^{65}Cu^{2+}$ was added (ca. 5 μL) to the protein solution. Following metal addition, the pH was measured using a microprobe (Hanna Instruments, Italy) and readjusted to 7.4 using concentrated Na_2HPO_4 or to pH 5.0 using concentrated HCl. This resulted in final protein concentrations of 300−350 μM. Samples were then immediately transferred via pasteur pipet to a quartz EPR tube (Wilmad), snap frozen in liquid nitrogen, and transferred to −80 °C storage until use. Tubes were transported to the EPR facility on dry ice.

Continuous-Wave EPR Spectroscopy. EPR experiments were carried out at X-band with a Bruker ESP380E spectrometer, using either a Bruker ER 4118 cylindrical dielectric resonator inserted in an Oxford Instruments CF935 cryostat or with a quartz coldfinger insert in a rectangular TE_{012} cavity (Bruker). Microwave frequencies were measured with an EIP Microwave 548A frequency counter. Experimental conditions were as follows: microwave power, 10 mW; microwave frequency, 9.42 GHz; modulation amplitude, 4 G; temperature, 77 K; sweep time, 84 s; time constant, 81.92 ms; 8 averages. Second derivative spectra were obtained by differentiating the usual first harmonic spectrum, followed by Fourier filtering using a Hamming window to remove high frequency noise. Where multiple species were present, the percentage of Cu^{2+} in each binding mode was determined by isolation and normalization of its first-derivative EPR spectrum by double integration.

EPR simulations were performed using version 1.1.4 of the XSophe simulation package[34] on an i686 PC running Mandriva 2007. All simulations used exact matrix diagonalization to determine the main transitions in conjunction with high-order perturbation theory to further solve for the electron−nuclear superhyperfine (shf) transitions. Distributions of the principal g and A parameters of ^{65}Cu were also included using the g and A strain line width model.[35] Simulations of shf parameters were simplified by assuming coupling of ^{65}Cu to equivalent nitrogen nuclei. Independent coupling constants for each nitrogen were trialed but did not improve the fit. Approximating each nitrogen to possess a similar coupling constant is a common assumption and sufficient for determining the number of directly coordinated nitrogen-based ligands. For example, three equivalent nitrogens with isotropic shf parameters were used to simulate and reproduce shf spectra derived from Cu^{2+} coupling to chemically inequivalent nitrogen ligand nuclei in the prion protein octapeptide.[36]

Pulsed EPR Spectroscopy. Pulsed EPR experiments were carried out at 2 K using the ESP380E spectrometer fitted with a Bruker ER 4118 cylindrical dielectric resonator, an Oxford Instruments CF935 cryostat, and a 1 kW TWT amplifier. The microwave frequency was measured with an EIP microwave 548A frequency counter. Echo-detected EPR (ED-EPR) spectra were acquired by recording the peak amplitude of a Hahn echo (obtained using the pulse sequence $\pi/2-\tau-\pi-\tau-$echo) as a function of the magnetic field.

Orientation-selective hyperfine sublevel correlation (HYSCORE) spectroscopy was carried out at a field corresponding to the maximum intensity of the ED-EPR spectrum, using a $\pi/2-\tau-\pi/2-t_1-\pi-t_2-\pi/2-\tau-$echo sequence, with pulse lengths $t_{\pi/2} = 16$ ns and $t_\pi = 24$ ns and $\tau = 144$ ns. For this choice of τ, the first blind spot[42] occurred at 6.94 MHz and hence the spectrum was effectively blind-spot free. Moreover, it also effectively suppressed modulation due to weakly coupled distant protons (ubiquitous in biological EPR samples) at the Larmor frequency of $\nu_p = 14.4$ MHz, thereby avoiding foldback of this frequency, which extended beyond the Nyquist limit of $\nu_N = 1/\Delta t = 7.81$ MHz. The time intervals t_1 and t_2 were varied from 48 to 8240 ns in steps of 64 ns, and an eight-step phase cycle was used to eliminate unwanted echoes. The real part of the time-domain spectra was processed by background subtraction using a second-order polynomial fit, zero-filling, and Hamming apodization. Absolute value spectra were then obtained following FFT, and the two-dimensional spectrum was symmetrized.

Results and Discussion

Cu^{2+} Binding Modes of α-Synuclein at pH 7.4. To determine whether multiple Cu^{2+} coordination modes were present in αS at physiological pH, we examined the Cu^{2+} binding of αS H50N to remove contributions from His-anchored coordination.[37] In Figure 1, the CW-EPR spectrum of the H50N mutant was compared with wt αS. It was evident that the $A_{||}$ hyperfine peaks of αS H50N were offset downfield with respect to the wt, in addition to a significant narrowing of its experimental line shape. This was consistent with the elimination of one or more overlapping Cu^{2+} binding spectra. In order to isolate other potential binding modes in the wt protein, a weighted subtraction of the H50N spectrum (Figure 1b) from the wt spectrum (Figure 1a) was therefore performed. The spectra isolated in Figure 1b and 1c were both characteristic of single species, suggesting that the wt protein at pH 7.4 binds Cu^{2+} via two independent coordination modes. The mode characterized by the H50N αS

(31) Cappai, R.; Leck, S. L.; Tew, D. J.; Williamson, N. A.; Smith, D. P.; Galatis, D.; Sharples, R. A.; Curtain, C. C.; Ali, F. E.; Cherny, R. A.; Culvenor, J. G.; Bottomley, S. P.; Masters, C. L.; Barnham, K. J.; Hill, A. F. *FASEB. J.* **2005**, *19*, 1377–1379.
(32) Marley, J.; Lu, M.; Bracken, C. *J. Biomol. NMR* **2001**, *20*, 71–75.
(33) Cai, M.; Huang, Y.; Sakaguchi, K.; Clore, G. M.; Gronenborn, A. M.; Craigie, R. *J. Biomol. NMR* **1998**, *11*, 97–102.
(34) Hanson, G. R.; Gates, K. E.; Noble, C. J.; Griffin, M.; Mitchell, A.; Benson, S. *J. Inorg. Biochem.* **2004**, *98*, 903–916.
(35) Pilbrow, J. R. *Transition Ion Electron Paramagnetic Resonance*; Clarendon Press: Oxford, 1990.
(36) Aronoff-Spencer, E.; Burns, C. S.; Avdievich, N. I.; Gerfen, G. J.; Peisach, J.; Antholine, W. E.; Ball, H. L.; Cohen, F. E.; Prusiner, S. B.; Millhauser, G. L. *Biochemistry* **2000**, *39*, 13760–13771.
(37) An Asp substitution was used instead of Ala to ensure the mutant retained a similar hydrophobicity to the wt.

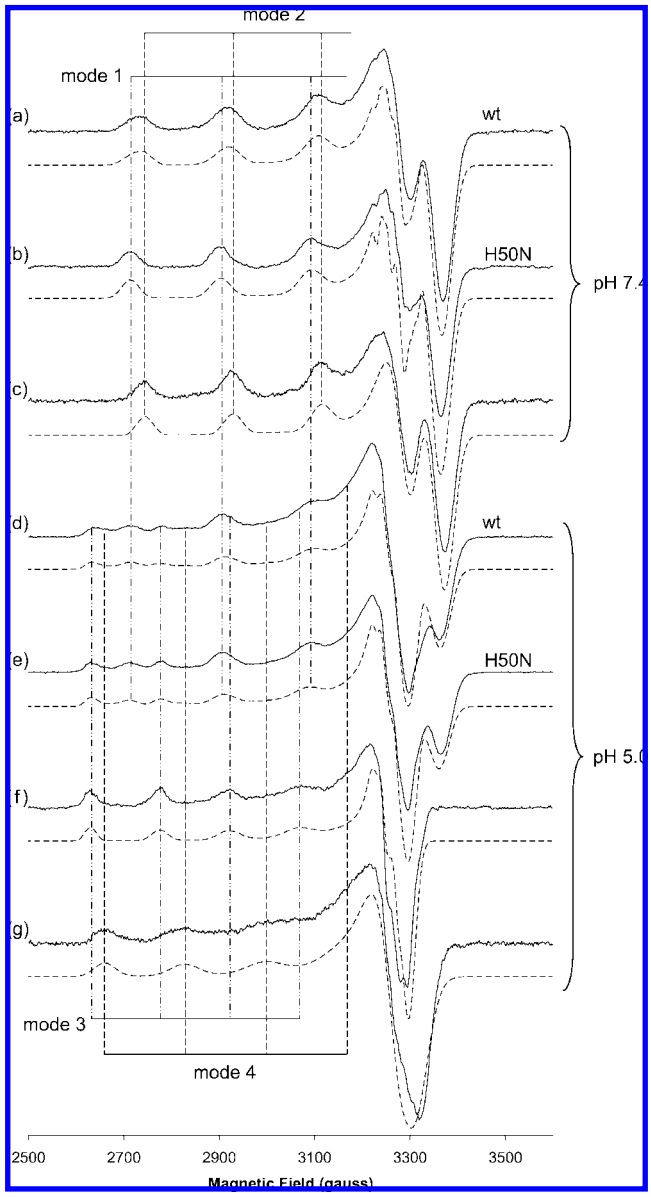

Figure 1. (—) Experimental and (---) simulated CW-EPR spectra of recombinant αS. (a) wt αS, pH 7.4 (45% mode 1, 55% mode 2); (b) αS H50N, pH 7.4 (100% mode 1); (c) Mode 2 spectrum isolated from a linear combination of 1.0 × (spectrum a) − 0.45 × (spectrum b); (d) wt αS, pH 5.0 (29% mode 1, 11% mode 2, 22% mode 3, 38% mode 4); (e) αS H50N, pH 5.0 (37% mode 1, 42% mode 3, 21% mode 4); (f) Mode 3 spectrum isolated from a linear combination of −0.70 × (spectrum b) + 0.13 × (spectrum c) − 1.92 × (spectrum d) + 3.49 × (spectrum e); (g) Mode 4 spectrum isolated from a linear combination of −0.37 × (spectrum b) − 0.37 × (spectrum c) + 3.70 × (spectrum d) – 1.96 × (spectrum e). Vertical lines indicate the position of resolved $A_{||}(^{65}Cu)$ hyperfine resonances belonging to different copper binding modes. All spectra are drawn with the same maximum peak-to-peak intensity for clarity. Percentages were determined following normalization of the EPR spectra. Spin Hamiltonian parameters characterizing each mode appear in Table 1 and the experimental conditions appear in Methods.

spectrum of Figure 1b will hereafter be referred to as "mode 1", while the coordination mode characterized by the residual spectrum in Figure 1c will be called "mode 2".

The EPR spectra of both modes were typical of type II Cu^{2+} centers with N and O ligands in a square-planar or tetragonal environment.[38] Quantification of Cu^{2+} binding by double integration of the EPR spectra revealed that a comparable proportion of Cu^{2+} was bound by modes 1 and 2 in wt αS (45% and 55%, respectively) under conditions of stoichiometric Cu^{2+} loading at pH 7.4. These findings contrast with an earlier study of full length αS, where the EPR spectrum at pH 6.5 was ascribed to a single Cu^{2+} mode (Table 1).[16]

The reduction in inhomogeneous broadening that resulted from using isotopically enriched ^{65}Cu resulted in the ability to resolve the ^{14}N shf structure in the $g_{\perp}$ region of mode 1 (Figure 1b). Upon differentiating this spectrum, this structure was made more readily apparent and mode 1 could be simulated by assuming magnetic coupling of Cu^{2+} with two equivalent nitrogen ligands (Table 1, Figure 2). To identify the residues involved, we noted that paramagnetic NMR studies of a similar αS H50A mutant clearly localized Cu^{2+} binding to the far N-terminus.[27] Moreover, our EPR spectrum of αS H50N was characterized by principal $g_{||}$ and $A_{||}$ parameters which closely paralleled those of the {NH_2, N^-, β-COO^-, H_2O} mode determined from spectroscopic and potentiometric studies of truncated model peptides αS(1−17), αS(1−28), αS(1−39) and NH_2-$M^{29}D^{30}$-56 (Table 1).[28,22,39] These two observations supported an assignment of mode 1 to a {NH_2, N^-, β-COO^-, H_2O} binding mode, involving coordination of the N-terminal amine of Met1 and the deprotonated backbone amide and carboxylate side chain of Asp2 (Figure 3a).

Although no ^{14}N shf structure could be resolved in Figure 1c, the principal $g_{||}$ and $A_{||}$ parameters of mode 2 (Table 1) suggested a 2N1O or 3N1O coordination sphere.[38] To attempt to resolve metal−ligand interactions from the Cu^{2+} binding in mode 2, uniformly ^{15}N-labeled αS (>98% ^{15}N) was examined. Since ^{15}N has a lower nuclear spin and 40% larger nuclear magnetic moment compared with ^{14}N, the shf structure will be characterized by fewer lines that are more widely spaced. Figure 4 shows that the resolution of shf interactions was visibly improved for ^{15}N-labeled αS compared with the natural abundance (>99% ^{14}N) spectrum. Since only mode 1 showed evidence of the shf structure in the natural abundance spectra, we first simulated mode 1 using the same parameters as before (Table 1, Figures 1b, 2), but with $A_{iso}(^{15}N) = 1.40 \times A_{iso}(^{14}N)$ to account for the larger magnetic moment of the ^{15}N nucleus. A weighted contribution from the mode 2 simulation (Figure 1c, Table 1), where no shf coupling was included, was then added. If the ^{15}N-labeled spectrum could be reproduced in this fashion, then it could be concluded that the metal−ligand couplings from mode 2 Cu^{2+} binding still remained unresolved. The simulation in Figure 5 indicated that this was indeed the case, indicating that no additional information regarding mode 2 could be obtained using CW-EPR at X-band. Nevertheless, the ^{15}N-labeling provided additional confirmation of the assignment of a 2N2O coordination sphere to mode 1.

While the number of nitrogen ligands in mode 2 Cu^{2+} binding could not be determined, the coordination of His50 could be identified by using electron spin−echo envelope modulation (ESEEM) spectroscopy. The ESEEM spectra of systems with imidazole coordination from His side chains are well understood.[40,41] At X-band frequencies, approximate cancelation of the nuclear Zeeman and electron-nuclear hyperfine interactions takes place, and modulation frequencies characteristic of single-quantum (ν_0, ν_-) and double-quantum (ν_+, ν_{dq}) transitions appear in the 0−4 MHz range.[40,42] The transitions within the α electron spin manifold give rise to frequencies ν_0, ν_-, and ν_+, whereas ν_{dq}

(38) Peisach, J.; Blumberg, W. E. *Arch. Biochem. Biophys.* **1974**, *165*, 691–698.
(39) Kowalik-Jankowska, T.; Rajewska, A.; Wiśniewska, K.; Grzonka, Z.; Jezierska, J. *J. Inorg. Biochem.* **2005**, *99*, 2282–2291.

Table 1. Spin Hamiltonian Parameters of Cu^{2+} Binding Modes Identified in Recombinant αS under Various Conditions and Their Comparison with Other Work[a,b]

system	$g_{\|}$	$g_{\perp}$	$A_{\|}(^{63}Cu)$	$A_{\perp}(^{63}Cu)$	$A_{\|}(^{14}N)$	$A_{\perp}(^{14}N)$	coordination[c]	pH	ref
"mode 1"									
αS(1−140) wt, H50N	2.246	2.054	185	15.0	11.0	13.5	2N2O	5.0, 7.4	[d]
"mode 2"									
αS(1−140) wt	2.228	2.050	179	n.d.[e]	n.d.	n.d.	2N2O/3N1O[f]	7.4	[d]
"mode 3"									
αS(1−140) wt, H50N	2.363	2.066	150	10.3	10.0	11.0	1N3O	5.0	[d]
"mode 4"									
αS(1−140) wt, H50N	2.313	2.069	168	n.d.	n.d.	n.d.	4O[f]	5.0	[d]
"{NH_2, N^-, β-COO^-, H_2O}"									
M^{29}-D^{30}-56[g]	2.242	n.d.	193	n.d.	n.d.	n.d.	2N2O	5.5	28
M^{26}-D^{27}-56 (A30P,A53T)[h]	2.230	n.d.	188	n.d.	n.d.	n.d.	2N2O	5.5	22
αS (1−17)	2.249	n.d.	193	n.d.	n.d.	n.d.	2N2O	4.0, 6.5, 8.8	39
αS (1−28)	2.247	n.d.	193	n.d.	n.d.	n.d.	2N2O	4.0, 6.5, 8.5	39
αS (1−39)	2.246	n.d.	192	n.d.	n.d.	n.d.	2N2O	4.5,6.5, 8.5	39
αS (1−39) A30P	2.245	n.d.	194	n.d.	n.d.	n.d.	2N2O	4.5, 6.5, 8.5	39
"{NH_2, N^-, β-COO^-, N_{Im}}"									
M^{29}-D^{30}-56[g]	2.226	n.d.	184	n.d.	n.d.	n.d.	3N1O	7.0	28
M^{26}-D^{27}-56 (A30P,A53T)[h]	2.228	n.d.	186	n.d.	n.d.	n.d.	3N1O	7.5	22
"{N_{Im},$2N^-$}"									
Ac-M^{29}-D^{30}-56	2.226	n.d.	173	n.d.	n.d.	n.d.	3N1O	7.5	28
other									
αS (1−140)[i]	2.223	2.05	186	n.d.	n.d.	n.d.	2N2O	5.0, 6.5	16
αS (1−140) DEPC-modified	2.316	2.06	176	n.d.	n.d.	n.d.	4O	6.5	16

[a] All hyperfine parameters are expressed in units of 10^{-4} cm^{-1}. [b] Where hyperfine data are given in gauss (G) in the original reference, it has been converted into wavenumber using the expression $A_{\|}$ [$10^{-4}cm^{-1}$] = $10^4(g_{\|}\beta_e/hc) \times A_{\|}$ [G], where h is Plank's constant, $c = 2.9979 \times 10^{10}$ cm·s^{-1} and $\beta_e = 9.274 \times 10^{-28}$ J·G^{-1}. [c] Where ^{14}N hyperfine couplings are tabulated, the coordination has been determined from empirical simulation of the shf structure by assuming coupling to equivalent nitrogen nuclei. Otherwise, the coordination has been determined as described in the original reference. [d] This work. To aid comparison with other work in which natural abundance copper (69% ^{63}Cu, 31% ^{65}Cu) has been used, hyperfine couplings have been converted from ^{65}Cu to those expected for ^{63}Cu by noting that its magnetic moment is larger by a factor of $|g_n(^{65}Cu)/g_n(^{63}Cu)| = 1.07$. The uncertainty in g and A values is estimated to be ± 0.001 and $\pm 1 \times 10^{-4}cm^{-1}$, respectively. [e] n.d. = not determined. [f] Coordination estimated using Blumberg−Peisach diagrams (ref 38). [g] M^{29}-D^{30}-56: NH_2-M^{29}-D^{30}-GKTKEGVLYV^{40}GSKTKEGVVH^{50}GVATVA^{56}-NH_2. [h] M^{26}-D^{27}-56 (A30P,A53T): NH_2-M^{26}-D^{27}-EA*P*GKTKEGVLYV^{40}GSKTKEGVVH^{50}GV*T*TVA^{56}-NH_2. [i] Parameters obtained by assuming a single binding mode present at pH 6.5.

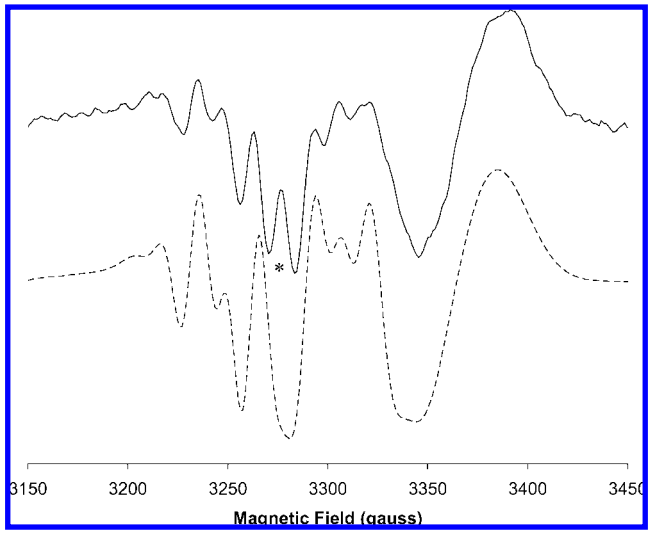

Figure 2. Analysis of the second derivative CW-EPR spectrum of αS H50N, obtained by differentiating the spectrum in Figure 1b. (—) Experimental spectrum expanded about the $g_{\perp}$ region; (---) Simulation assuming $^{65}Cu^{2+}$ coupling with two directly coordinated ^{14}N nuclei. The lines flanking the asterisk in the experimental spectrum partially overlap in the simulation. Spin Hamiltonian parameters are given in Table 1. Line width parameters: $\Delta g_{\|}/g_{\|} = 0.007$, $\Delta g_{\perp}/g_{\perp} = 0.0021$, $\Delta A_{\|} = -5.0 \times 10^{-4}$ cm^{-1}, $\Delta A_{\perp} = 0$, residual line width = 5.0×10^{-4} cm^{-1}.

derives from the β manifold. In two-dimensional ESEEM spectroscopy, the double quantum frequencies appear as cross-peaks. Figure 6 shows a 2D ESEEM (HYSCORE) spectrum of wt αS at pH 7, with cross-peaks at ∼(1.6, 4.0) MHz being a diagnostic of distal imidazole ^{14}N coordination by His50. The H50N mutant was also probed using HYSCORE, and as expected, the cross-peaks were absent. These results clearly confirmed the participation of His50 in Cu^{2+} binding via mode 2.

Folding of the Holo-Protein in Its Native Conformation. The principal $g_{\|}$ and $A_{\|}$ parameters of mode 2 in full length αS were similar to those of the dominant Cu^{2+} binding mode in the NH_2-$M^{29}D^{30}$-56 model fragment at pH 7.4 (Table 1), which was suggested to form a macrochelate involving Met1, Asp2, and His50 in a {NH_2, N^-, β-COO^-, N_{Im}} mode (Figure 3b).[28,43] However, in comparison with the truncated fragments, it is unclear whether the formation of a macrochelate in the full length protein would be entropically favorable due to the presence of an additional 28 residues separating the N-terminal amino group and His50.

Supporting evidence for macrochelate formation comes from the dependence of the relative proportions of mode 1 and 2 binding on protein length. Potentiometric and spectroscopic studies of the NH_2-$M^{29}D^{30}$-56 fragment indicated <5% popula-

(40) Deligiannakis, Y.; Louloudi, M.; Hadjiliadis, N. *Coord. Chem. Rev.* **2000**, *204*, 1–112.
(41) McCracken, J.; Pember, S.; Benkovic, S. J.; Villafranca, J. J.; Miller, R. J.; Peisach, J. *J. Am. Chem. Soc.* **1998**, *110*, 1069–1074.
(42) Schweiger, A.; Jeschke, G. *Principles of Pulse Electron Paramagnetic Resonanc*; Oxford University Press: Oxford, 2001.
(43) Interestingly, ref 27 was cited in support of the assignment of a {NH_2, N^-, β-COO^-, N_{Im}} coordination mode for full length αS, although the latter study concluded that such a coordination mode did not exist.

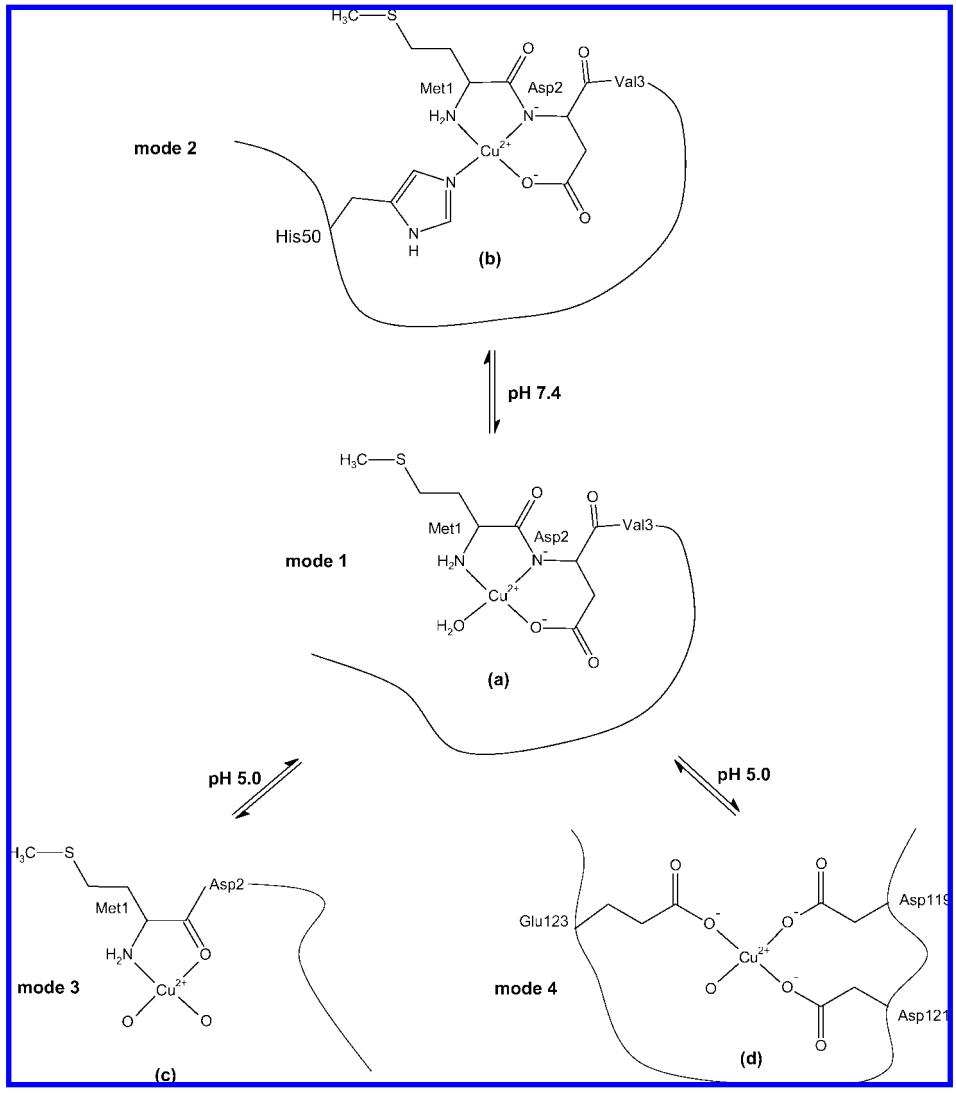

Figure 3. Two-dimensional representation of the putative Cu^{2+} binding modes of αS between pH 5.0 and 7.4. (a) The {NH_2, N^-, β-COO^-, H_2O} binding mode assigned to mode 1, observed at both pH 7.4 and 5.0, involving Met1 and Asp2. (b) One of the proposed binding modes assigned to mode 2, observed at pH 7.4, involving a macrochelate. The participation of His50 in mode 2 is confirmed by ESEEM spectroscopy (Figure 6); however the identity of the remaining ligands remains unclear. It is possible that mode 2 in the full-length protein involves not a macrochelate but rather {N_{im}, $2N^-$} coordination involving His50 and neighboring Val residues (see text). (c) The {NH_2, CO} binding mode assigned to mode 3, observed at pH 5.0, involving Met1 and unidentified oxygen ligands, potentially water molecules. (d) The 4O coordination mode assigned to mode 4, observed at pH 5.0, involving the carboxylate oxygens of Asp119, Asp121, and Glu123 side chains. The fourth oxygen ligand might be either the side-chain carbonyl of Asn123 or a water molecule.

tion of the {NH_2, N^-, β-COO^-, H_2O} mode and >95% coordination via the {NH_2, N^-, β-COO^-, N_{Im}} mode at pH 7.4.[28] Analogous studies of αS(1−17), αS(1−28), and αS(1−39) fragments indicated that when competition from His-anchored binding was eliminated, {NH_2, N^-, β-COO^-, H_2O} binding was present over pH 4−9 and accounted for essentially all of the Cu^{2+} species at pH 7.4. In comparison, the present study of the full length protein showed that the {NH_2, N^-, β-COO^-, H_2O} binding (mode 1) accounted for 45% of the bound Cu^{2+} at pH 7.4, which may be viewed as an intermediate between the above two extremes. This suggests that the equilibrium between the "N_{Im} -bound" (cf. mode 2) and "N_{Im}-unbound" (cf. mode 1) Cu^{2+} coordination modes shifts in favor of mode 1 as the number of residues separating the N-terminal amino group and the His ligand increases.

Evidence against a {NH_2, N^-, β-COO^-, N_{Im}} binding mode can be gleaned from studies of the Ac-$M^{29}D^{30}$-56 fragment, where binding via the N-terminal amine was inhibited.[28] Here the dominant binding mode between pH 7−8 was suggested to

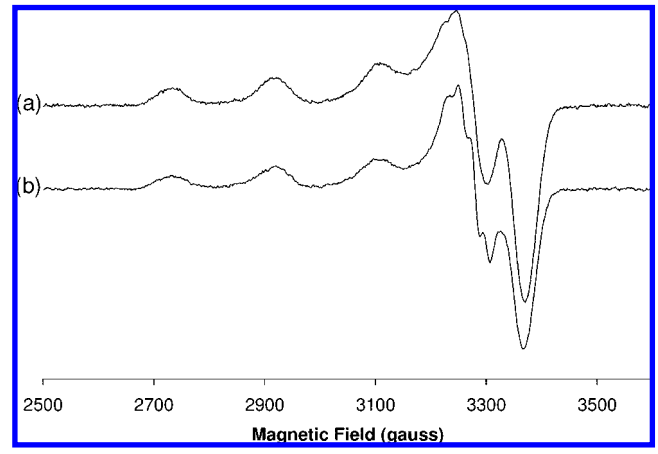

Figure 4. CW-EPR spectra of (a) wt αS and (b) ^{15}N-labeled wt αS in PBS 7.4 with 1 equiv of $^{65}CuCl_2$, showing the improved resolution of the metal−ligand shf structure following isotopic enrichment.

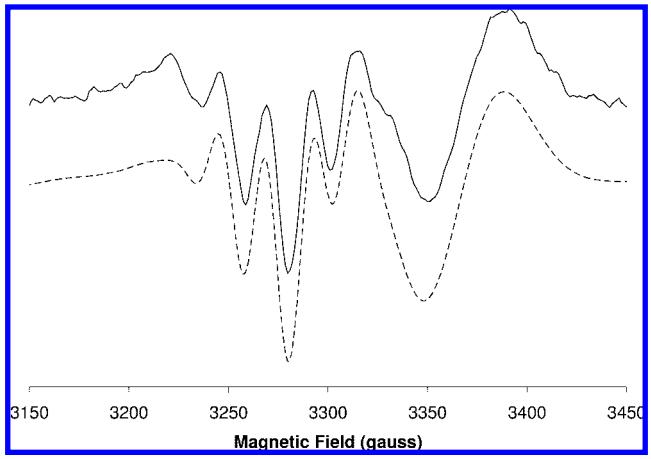

Figure 5. Analysis of the second derivative CW-EPR spectrum of ^{15}N-labeled wt αS, obtained by differentiating the spectrum in Figure 4b. (—) Experimental spectrum expanded about the $g_\perp$ region; (---) Simulation employing a weighted summation of mode 1 (45%) and mode 2 (55%), using the same parameters determined from the ^{14}N simulations (Table 1; Figures 1b and 2). The mode 1 simulation used an isotropic coupling constant $A_{iso}(^{15}N) = 1.40 \times A_{iso}(^{14}N)$ to account for the larger magnetic moment of the ^{15}N nucleus. The good fit of the experimental spectrum without the need to include shf interactions for mode 2 indicated that they remained unresolved in the ^{15}N-labeled protein.

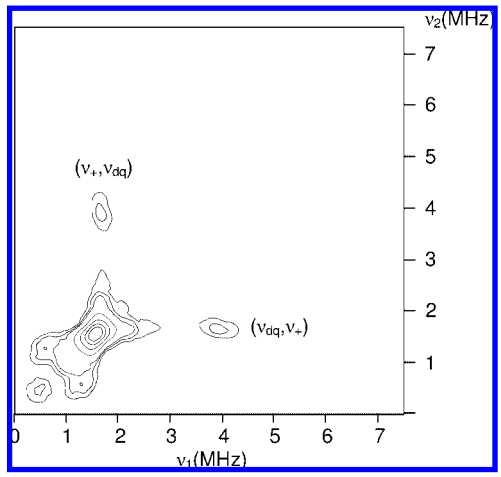

Figure 6. HYSCORE spectrum of wt αS in PBS pH 7 with 1 equiv of $^{65}CuCl_2$ at an external magnetic field corresponding to the maximum absorption in the $g_\perp$ region. Double-quantum frequencies ν_+ and ν_{dq}, related to the quadrupole interaction of the distal imidazole nitrogen nucleus, confirm Cu^{2+} binding to the side chain of His50. Experimental conditions: microwave frequency, 9.70 GHz; temperature, 2 K; $t_{\pi/2} = 16$ ns; $t_\pi = 24$ ns; $\tau = 144$ ns, $t_{10} = t_{20} = 48$ ns, $\Delta t_1 = \Delta t_2 = 64$ ns, repetition rate, 1 kHz.

be $\{N_{Im}, 2N^-\}$ and was characterized by principal $g_{||}$ and $A_{||}$ parameters that are also very close to those of mode 2 (Table 1). The likely amide donor atoms in this instance were proposed to be provided by His and Val residues,[28] which would compare well with the disappearance of backbone resonances from Val48 and Val52 observed from NMR spectra in the presence of a stoichiometric excess of Cu^{2+}.[27] Additional evidence opposing macrochelate formation comes from NMR studies, where the methanethiosulfonate spin label (MTSL) covalently attached at position 50 of αS H50C failed to induce paramagnetic broadening of NMR signals from residues at the N-terminus of the apoprotein.[27] However, it is unclear whether attachment of a bulky spin label at position 50 could sterically inhibit the protein from folding back on itself to enable close proximity of Met1 and His50.

If macrochelate formation is not favored in the full length protein, then the Ac-$M^{29}D^{30}$-56 model fragment may represent a better model of mode 2 coordination than its NH_2-$M^{29}D^{30}$-56 counterpart. The present EPR data cannot differentiate between $\{N_{Im}, 2N^-\}$ and $\{NH_2, N^-, \beta\text{-}COO^-, N_{Im}\}$ or even the simultaneous presence of both binding modes in the full-length protein.[44] Unequivocal assignment of the coordinating ligands in mode 2 using magnetic resonance techniques will require further isotopic labeling strategies.

Cu^{2+} Binding Modes of α-Synuclein at pH 5.0. Previous NMR spectroscopic investigation identified the onset of Cu^{2+} binding by the acidic C-terminus of αS at pH 5.0, where it appeared to be centered predominantly on Asp121.[16] CW-EPR indicated that N-terminal binding persisted at low pH (identified here as mode 2) in addition to other underlying spectral component(s) which were attributed to C-terminal binding. The characterization of the latter relied upon DEPC-treatment of wt αS at pH 6.5 to reduce competitive binding from other Cu^{2+} coordination modes.[16] On the other hand, the use of DEPC to isolate this binding introduced some uncertainty as to the validity of the derived EPR spectrum, because DEPC was shown to be capable of nonspecifically inhibiting nitrogen coordination by many amino acids in the wt protein.[27]

In order to investigate the nature of the Cu^{2+} binding of αS at low pH, EPR spectra of both wt and H50N αS were obtained at pH 5.0 (Figure 1d,e). The contribution from mode 2 was heavily diminished (from 55% to 11%) due to protonation of the proximal imidazole N, leading to similar EPR spectra for both wt and H50N αS. Mode 1 binding persisted at pH 5.0, but in conjunction with new Cu^{2+} binding modes, which will be referred to as "mode 3" and "mode 4". By careful algebraic manipulations of the spectra in Figure 1b−e, these modes could be spectrally isolated as shown in Figure 1f,g. Spin quantitation by double integration of the EPR spectra showed that, at pH 5.0, wt αS bound 1 equiv of Cu^{2+} in the ratio 29% mode 1, 11% mode 2, 22% mode 3, and 38% mode 4. The pH 5.0 spectrum of the H50N mutant was comprised of 37% mode 1, 42% mode 3, and 21% mode 4.

A comparison of the principal $g_{||}$ and $A_{||}$ parameters of mode 3 (Table 1) with the Blumberg−Peisach diagrams suggested either a 1N3O or 4O metal coordination sphere.[38] However, mode 3 showed evidence of a hyperfine structure in the $g_\perp$ region, which could not be reproduced by simulations involving $A_\perp(^{65}Cu)$ splittings alone but required the introduction of isotropic coupling to a single ^{14}N nucleus (Figures 1f and 7, Table 1). At pH 5.0, deprotonation of a backbone amide group was unfeasible, and hence the likely source of nitrogen coordination was the N-terminal amine. Potentiometric and circular dichroism data obtained within pH 3.5−4.5 have suggested an $\{NH_2, CO\}$ or an $\{N_{Im}\}$ coordination mode in truncated N-terminal fragments.[28,39] The latter possibility could automatically be ruled out for the full length protein, due to the presence of mode 3 in the H50N mutant. Hence mode 3 is suggested to form a $\{NH_2, CO\}$ coordination mode involving Met1 (Figure 3c).

The $g_{||}$ and $A_{||}$ parameters of mode 4 were indicative of 4O coordination[38] and very close to those previously determined

(44) The latter possibility would imply Figure 1c was comprised of two overlapping spectra, which might explain the absence of shf structure in this instance.

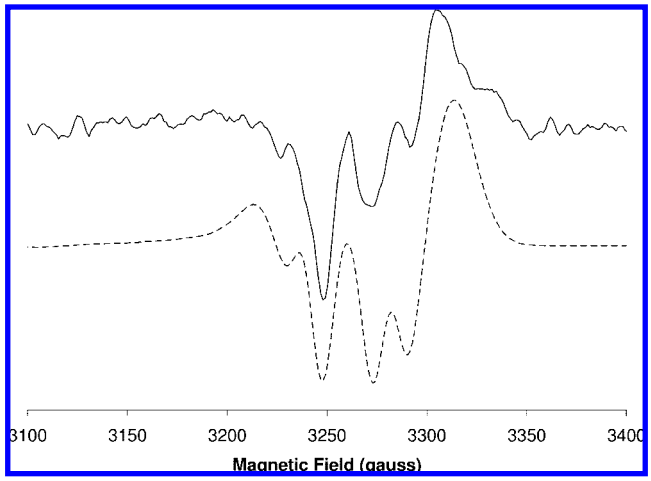

Figure 7. Analysis of the second derivative CW-EPR spectrum of mode 3, obtained by differentiating the spectrum in Figure 1f. (—) Experimental spectrum expanded about the $g_\perp$ region; (---) simulation assuming $^{65}Cu^{2+}$ coupling with one directly coordinated ^{14}N ligand nucleus. The splittings in this region could not be reproduced by ^{65}Cu nuclear hyperfine interactions alone. Simulation parameters are given in Table 1. Line width parameters: $\Delta g_{||}/g_{||} = 0.0070$, $\Delta g_\perp/g_\perp = 0.0024$, $\Delta A_{||} = -8.0 \times 10^{-4}$ cm^{-1}, $\Delta A_\perp = 0$; residual line width $= 5.0 \times 10^{-4}$ cm^{-1}.

for DEPC-treated αS (Table 1), where Cu^{2+} binding occurred predominantly in the vicinity of residues 119−121.[16] Mode 4 is therefore attributed to a coordination mode of this type (Figure 3d). Although DEPC was shown to inhibit Cu^{2+} binding at the N-terminus in addition to His50,[27] it is noteworthy that DEPC-treated αS also showed evidence of a ^{14}N shf structure.[16] This structure can now be explained by an incomplete blocking of the N-terminal amine by DEPC, leading to the presence of a residual Cu^{2+} binding signal from mode 3.

Although simulated as a single species, the width and asymmetry of the low-field $A_{||}$ resonances of mode 4 (Figure 1g) suggested the spectrum was comprised of more than one species. However, additional binding modes could not be isolated from the available spectra. Since NMR data suggested additional Cu^{2+} binding, albeit to a lesser extent, in the vicinity of Asp135 at pH 5.0,[16] overlapping signals in Figure 1g may arise from weaker Cu^{2+} binding centered upon this residue. Additional studies employing isotopic enrichment schemes and/or site-directed mutagenesis would be required to confirm these assignments.

Conclusions

EPR spectroscopy, in conjunction with site-directed mutagenesis and isotopic labeling, was used to identify a minimum of four Cu^{2+} binding modes adopted by full length human αS between pH 5.0−7.4. One binding mode at pH 7.4 was isolated by introducing an H50N mutation (mode 1). Spectral simulations of mode 1 revealed a 2N2O coordination sphere whose spin Hamiltonian parameters were in close agreement with those observed for the {NH_2, N^-, β-COO^-, H_2O} binding mode involving Met1 and Asp2 in truncated model peptides. By careful algebraic spectral subtraction, a second spectral component at pH 7.4 was isolated (mode 2), in which pulsed EPR spectroscopy confirmed the involvement of the single histidine residue at position 50. Due to an unresolved shf structure, the number of nitrogen ligands could not be unambiguously determined for mode 2, although its spin Hamiltonian parameters were found to be close to both {NH_2, N^-, β-COO^-, N_{Im}} and {N_{Im}, $2N^-$} coordination modes proposed for the M_{29}-D_{30}-56 and Ac-M_{29}-D_{30}-56 fragments, respectively. While it would appear entropically unfavorable, it is suggested that no definitive evidence yet exists to rule out the formation of a {NH_2, N^-, β-COO^-, N_{Im}} macrochelate in the full length protein. At pH 5.0, the N_{Im}-anchored binding (mode 1) was strongly diminished, while mode 2 binding persisted in equilibrium with two new Cu^{2+} binding modes. These were carefully isolated from algebraic combinations of wt and H50N EPR spectra obtained at both pH 5.0 and pH 7.4. Resolution of ^{14}N shf structure in mode 3 enabled the simulation of a 1N3O Cu^{2+} coordination sphere, with the likely nitrogen donor originating from the terminal amino nitrogen in a {NH_2, CO} binding mode suggested from model complexes (mode 3). A Cu^{2+} binding mode similar to that previously identified in DEPC-modified αS was also observed at pH 5.0 (mode 4) and attributed to C-terminal Cu^{2+} binding anchored around Asp121 and possibly Asp135. Taken as a whole, these results correlate a number of disparate findings from earlier investigations of model fragments and the full length protein to better elucidate the copper binding properties of recombinant α-synuclein. Future investigations will be directed toward the determination of the individual binding affinities of modes 1 and 2, additional isotopic labeling schemes to further refine the coordination sphere of the above Cu^{2+} binding modes (particularly mode 2), and probing changes in coordination upon association with lipid membranes.

Acknowledgment. This work was supported by a Program Grant administered by the National Health and Medical Research Council of Australia. We thank Denise Cappai and Dr Cyril Curtain for technical assistance.

Supporting Information Available: Size-exclusion chromatogram and SDS-PAGE of the purified fraction of wt αS, ^{15}N-labeled αS and H50N αS (Figure S1). Complete author list for Polymeropoulos et al. (ref 4) and Kaur et al. (ref 23). This material is available free of charge via the Internet at http://pubs.acs.org.

JA800708X